Overexpression of VEGF-A in podocytes of adult mice causes glomerular disease

Delma Veron[1], Kimberly J. Reidy[2], Claudia Bertuccio[1], Jason Teichman[2], Guillermo Villegas[2], Juan Jimenez[3], Wa Shen[2], Jeffrey B. Kopp[4], David B. Thomas[5] and Alda Tufro[1]

[1]Department of Pediatrics, Yale University School of Medicine, New Haven, Connecticut, USA; [2]Department of Pediatrics, Albert Einstein College of Medicine, Bronx, New York, USA; [3]Analytical Imaging Facility, Albert Einstein College of Medicine, Bronx, New York, USA; [4]Kidney Disease Section, National Institute of Diabetes and Digestive and Kidney Diseases, National Institutes of Health, Bethesda, Maryland, USA and [5]Department of Pathology, Albert Einstein College of Medicine, Bronx, New York, USA

We sought to examine the pathogenic role of excessive VEGF-A expression in podocytes, since it has been reported that diabetic nephropathy and other glomerular diseases are associated with increased VEGF-A expression. The induction of podocyte-specific VEGF164 overexpression in adult transgenic mice led to proteinuria, glomerulomegaly, glomerular basement membrane thickening, mesangial expansion, loss of slit diaphragms, and podocyte effacement. When doxycycline-mediated VEGF164 was stopped, these abnormalities reversed. These findings were associated with reversible downregulation of metalloproteinase 9 and nephrin expression. Using transmission electron microscopy, we established that VEGF-A receptor-2 (VEGFR2) was expressed in podocytes and glomerular endothelial cells. We also found that VEGF164 induced VEGFR2 phosphorylation in podocytes. Further, we were able to co-immunoprecipitate VEGFR2 and nephrin using whole kidney lysates, confirming interaction *in vivo*. This implies that autocrine and paracrine VEGF-A signaling through VEGFR2 occurs in podocytes and may mediate the glomerular phenotype caused by VEGF164 overexpression. Thus, we suggest that podocyte VEGF164 overexpression in adult mice is sufficient to induce glomerular filtration barrier structural and functional abnormalities similar to those present in murine diabetic nephropathy.

Kidney International (2010) **77,** 989–999; doi:10.1038/ki.2010.64; published online 10 March 2010

KEYWORDS: diabetic glomerulopathy; nephrin; podocyte; proteinuria; VEGF

Correspondence: *Alda Tufro, Department of Pediatrics, Yale University School of Medicine, 333 Cedar Street, P.O. Box 208064, New Haven, Connecticut 06520–8064, USA. E-mail: alda.tufro@yale.edu*

Received 6 October 2009; revised 2 January 2010; accepted 13 January 2010; published online 10 March 2010

Vascular endothelial growth factor-A (VEGF-A) is the major determinant and regulator of angiogenesis.[1] Inactivation of a single VEGF-A allele causes embryonic lethality, showing that threshold levels of VEGF-A signaling are required for maintaining the differentiation, correct assembly, and maturation of endothelial cells.[2,3] Similarly, podocyte-specific deletion of VEGF-A in mice showed that over 50% allelic dose of VEGF-A is required for development and maintenance of a functional glomerular filtration barrier.[4] Conversely, massive VEGF-A overexpression in podocytes caused glomerular collapse and perinatal lethality.[4] These developmental phenotypes precluded the analysis of the role of VEGF-A expression in adult kidney disorders.

Excessive renal VEGF-A expression has been documented in diabetic nephropathy and glomerular diseases, which are the leading causes of end-stage renal disease in humans.[5] However, it is not clear whether changes in VEGF-A expression are a cause, a consequence, or a bystander in kidney diseases.[5–7] Anti-VEGF antibody therapy reduced the severity of diabetic nephropathy in rodents,[8–10] whereas it induced hypertension and glomerular disease in cancer patients.[11,12] VEGF-A was shown to accelerate the resolution of experimental glomerulonephritis, ameliorate cyclosporine nephropathy, and protect remnant kidneys.[13] Our previous *in vitro* studies showed that VEGF-A attracts endothelial cells to developing glomeruli,[14] promotes podocyte survival through an autocrine pathway involving VEGF receptor-2 (VEGFR2), induces podocin upregulation and its association with CD2AP.[15] It is unclear whether autocrine podocyte VEGF-A signaling occurs *in vivo*. In this study we report that induction of moderate podocyte $VEGF_{164}$ overexpression in adult mice causes a glomerular disease characterized by glomerulomegaly, mesangial proliferation, glomerular basement membrane (GBM) thickening, loss of slit diaphragms, podocyte effacement, and proteinuria in the absence of a diabetic milieu, which is reversible upon removal of doxycycline, and we provide insight into its molecular mechanism.

RESULTS

Inducible podocyte $VEGF_{164}$ overexpression *in vivo*

To analyze the pathogenic role of VEGF-A in glomerular disease and circumvent early lethality, we developed an inducible, podocyte-specific, tetracycline-regulated $VEGF_{164}$ overexpression model (*podocin-rtTA:tet-O-VEGF*$_{164}$) by breeding *podocin-rtTA* mice[16] with *tet-O-VEGF*$_{164}$ mice.[17] In *podocin-rtTA:tet-O-VEGF*$_{164}$ mice, immunoreactive VEGF-A localized to podocytes was increased upon doxycycline induction (Supplementary Figure S1a). VEGF-A protein in whole kidney lysate measured by enzyme-linked immunosorbent assay increased twofold in doxycycline-treated *podocin-rtTA:tet-O-VEGF*$_{164}$ mice (0.1 ± 0.005 vs 0.2 ± 0.01 pg/μg protein, −dox, $n = 8$ vs + dox, $n = 13$, $P < 0.05$, Supplementary Figure S1b), whereas urine VEGF-A increased 15-fold (13.1 ± 1.2 vs 206.7 ± 110.2 pg/day, −dox, $n = 9$ vs + dox, $n = 6$, $P < 0.05$).

Podocyte $VEGF_{164}$ overexpression causes proteinuria

Adult mice overexpressing podocyte $VEGF_{164}$ for 1 month developed proteinuria (TOPO + dox, Figure 1a–c). In contrast, age-matched uninduced *podocin-rtTA:tet-O-VEGF*$_{164}$ mice (TOPO −dox) did not develop proteinuria (Figure 1a and c), nor did single transgenic mice receiving doxycycline (CON + dox, Figure 1a), indicating that neither the transgenes nor the doxycycline *per se* caused proteinuria. Notably, $VEGF_{164}$-induced proteinuria was reversible 2 weeks after doxycycline removal from the diet (Figure 1b and c), suggesting a cause-and-effect relationship between $VEGF_{164}$ and proteinuria. Moreover, proteinuria positively correlated with increased kidney VEGF-A content in mice overexpressing $VEGF_{164}$ (Figure 1d), but did not correlate with VEGF-A plasma levels, which remained unchanged (24 ± 1.9 vs 22 ± 2.2 pg/ml, −dox, $n = 9$ vs + dox, $n = 12$, $P =$ NS), suggesting that podocytes are not the main source of circulating VEGF-A, and that podocyte $VEGF_{164}$ effects are local rather than systemic. $VEGF_{164}$-induced albuminuria was detected by immunoblotting (Figure 1c), and quantified by enzyme-linked immunosorbent assay (Figure 1e). The urine albumin/creatinine ratio was 4- to 16-fold higher in doxycycline-induced than in uninduced *podocin-rtTA:tet-O-VEGF*$_{164}$ mice ($P = 0.0027$, Figure 1e), consistent with the data obtained by dipstick and western analysis.

Podocyte $VEGF_{164}$ overexpression induces glomerulomegaly

We examined the morphologic changes associated with $VEGF_{164}$-induced proteinuria. Podocyte $VEGF_{164}$ overexpression in adult mice induced glomerular enlargement, thickened GBM, and mild mesangial expansion (Figure 2a, Supplementary Figure S2a). Morphometric analysis confirmed $VEGF_{164}$-induced glomerulomegaly, with 1.8- to 2-fold increase in mean glomerular volume, which was partially reversible upon cessation of $VEGF_{164}$ overexpression (Figure 2a and b), and showed a right shift in the distribution of glomerular volumes indicating widespread enlargement and increased size heterogeneity (Figure 2b) and increased mesangial matrix area (Supplementary Figure S2a).

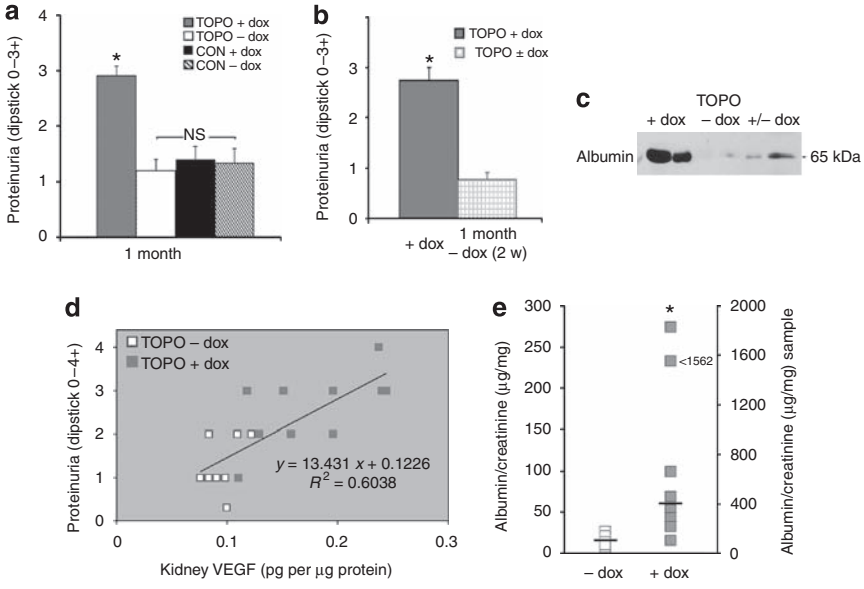

Figure 1 | Podocyte $VEGF_{164}$ overexpression in adult mice causes proteinuria. (**a**) *Podocin-rtTA:tet-O-VEGF*$_{164}$ adult mice induced with doxycycline for 1 month (TOPO + dox) develop proteinuria, as compared with uninduced *podocin-rtTA:tet-O-VEGF*$_{164}$ mice (TOPO −dox) and single transgenic controls receiving doxycycline or not (CON + dox and CON −dox). (**b**) Proteinuria is reversible upon removal of doxycycline induction (TOPO + dox vs TOPO ± dox). (**c**) Albumin immunoblot showing albuminuria in induced TOPO + dox, no albuminuria in uninduced TOPO −dox, and minimal albuminuria in TOPO ± dox. (**d**) Proteinuria has a significant positive correlation with kidney vascular endothelial growth factor-A (VEGF-A) content in induced TOPO mice (+ dox), whereas it does not in uninduced TOPO mice (−dox). (**e**) Urine albumin/creatinine ratio (μg/mg) in TOPO + dox ($n = 8$) is more than fourfold higher than in TOPO −dox ($n = 6$). Notice that the scale on the right side of the figure is depicted to include the sample labeled (<), which showed 1562 μg/mg, and horizontal bars depict the median for each experimental group. In all graphs *indicates $P < 0.05$ TOPO + dox vs TOPO −dox mice, and TOPO + dox vs TOPO ± dox mice.

Podocyte $VEGF_{164}$ overexpression induces GBM thickening and podocyte effacement in adult mice

To further evaluate these glomerular abnormalities, kidneys were examined by transmission electron microscopy (TEM) 1 month after $VEGF_{164}$ transgene induction. TEM revealed a dramatic increase in GBM thickness and irregularity, and absence of lamina rara interna and externa in kidneys overexpressing $VEGF_{164}$ (Figure 2c, panels C and F) when compared with controls: *podocin-rtTA:tet-O-VEGF$_{164}$* without doxycycline (Figure 2c, panels I and L) and single transgenics on doxycycline (Figure 2c, panels A, B, D, and E) or off doxycycline (Figure 2c, panels G, H, J, and K), which were all normal. In addition to the GBM changes, doxycycline-induced mice showed partial foot process effacement and fusion (Figure 2c, panels C and F), and increased mesangial matrix deposition (Supplementary Figure S2b). These ultrastructural changes were observed in all kidneys examined and involved all glomeruli ($n \geqslant 3$/kidney). Surprisingly, no endothelial cell swelling or damage was observed by TEM and fenestrations were intact in kidneys from doxycycline-treated mice.

Morphometric analysis showed a twofold increase in GBM thickness in induced *podocin-rtTA:tet-O-VEGF$_{164}$* mice (TOPO +dox) when compared with uninduced controls (TOPO −dox, Figure 3a). Podocyte abnormalities were apparent along most of the GBM length, and resulted in an average 66% increase in foot process width (268 ± 5 vs 445 ± 28 nm, TOPO −dox vs TOPO +dox, $P < 0.001$), a 40% decrease in slit diaphragm density, and a threefold increase in occluding junction density (Figure 3b and c). $VEGF_{164}$-induced GBM, podocyte, and mesangial abnormalities were reversible at 2 weeks after doxycycline removal, underscoring the cause-and-effect relationship between excess podocyte VEGF-A and development of glomerular disease (Figure 3a–d, Supplementary Figure S1b).

We determined that random non-fasting plasma glucose levels were normal in *podocin-rtTA:tet-O-VEGF$_{164}$* on doxycycline (157 ± 24 mg/dl, $n = 8$), and not different from glucose levels in uninduced mice (179 ± 11 mg/dl $n = 9$, $P =$ NS). We also determined that systolic blood pressure was normal in doxycycline-induced and uninduced *podocin-rtTA:tet-O-VEGF$_{164}$* adult mice (104 ± 5 mm Hg, $n = 5$ vs 99 ± 5 mm Hg, $n = 5$, $P =$ NS).

Podocyte $VEGF_{164}$ overexpression decreases renal expression of matrix metalloproteinase 9 (MMP-9) and nephrin

GBM thickening and podocyte effacement are suggestive of abnormal GBM composition and altered podocyte protein expression,[18] respectively. Thus, we examined the expression of major GBM components and podocyte-specific proteins. We determined that collagen IV and laminin had similar localization in the glomerular and tubular GBM of mice overexpressing podocyte $VEGF_{164}$ and uninduced controls (Figure 4a). Real-time PCR revealed that collagen IV α3, α4, α5, and laminin α1, α5, and β1 kidney mRNA levels were unchanged after 1 month of $VEGF_{164}$ overexpression (Figure 4b). Similarly, Ndst1 and 2 and syndecan were unchanged (Figure 4b). Integrin α3 and α5 kidney mRNA levels did not change significantly, whereas integrin β1 mRNA was significantly decreased after 1 month of $VEGF_{164}$ overexpression (Figure 4b). However, β_1-integrin protein levels were not significantly altered (data not shown). In contrast, total kidney MMP-9 mRNA, protein level and activity, as well as glomerular immunoreactivity were decreased significantly in mice overexpressing podocyte $VEGF_{164}$ (Figure 4b, c, f, and g). MMP-9 downregulation was abrogated by removal of $VEGF_{164}$ induction (Figure 4c). As doxycycline is a known inhibitor of metalloproteinases,[19] we also examined the effect of doxycycline on renal MMP-9 expression in single transgenic mice (CON +dox). MMP-9 was not altered in single transgenics receiving doxycycline (Figure 4c and g). Hence, $VEGF_{164}$ overexpression specifically induced downregulation of MMP-9 expression and activity (Figure 5c and g). MMP-2 protein level remained unchanged in mice overexpressing podocyte $VEGF_{164}$ (Figure 5d). Collectively, these data suggest that podocyte $VEGF_{164}$ overexpression in adult mice reduces GBM turnover, as implied by the reversible decrease in MMP-9 mRNA, protein, and activity levels.

Podocyte $VEGF_{164}$ overexpression induced a significant decrease in nephrin mRNA, protein levels, and immunoreactivity, whereas nephrin phosphorylation increased them (Figure 4b, e, and f). Removal of doxycycline induction abrogated nephrin downregulation and phosphorylation, underscoring the cause–effect relationship between $VEGF_{164}$ overexpression and nephrin dysregulation (Figure 4e). In contrast, podocin expression levels remained unchanged (data not shown), suggesting that $VEGF_{164}$ overexpression does not cause overall dysregulation of slit diaphragm proteins or podocyte loss. The concomitant reversibility of nephrin downregulation and phosphorylation, podocyte effacement, and proteinuria upon removal of $VEGF_{164}$ induction suggests that nephrin dysregulation is the molecular basis for the $VEGF_{164}$-induced podocyte effacement.

Podocytes express VEGFR2, and VEGFR2 interacts with nephrin *in vivo*

We next analyzed whether the ultrastructural changes observed in podocytes from doxycycline-induced *podocin-rtTA:tet-O-VEGF$_{164}$* mice were caused by autocrine $VEGF_{164}$ signaling. We identified the glomerular cell types expressing VEGFR2, the main VEGF-A signaling receptor, by TEM and histochemistry in adult *Flk-1$^{+/-}$* mice, which carry one *Flk-1* allele with a *LacZ* gene in-frame insertion.[20] As shown in Figure 5a–c, *Flk-1$^{+/-}$* mice express β-Gal in lieu of VEGFR2 in both glomerular endothelial cells and podocytes. Moreover, β-Gal electron-dense precipitates were observed in the podocyte cell body (Figure 5b) and foot processes, closely adjacent to slit diaphragms (Figure 5c). Neighboring mesangial cells were mostly devoid of β-Gal electron-dense precipitates, and tubular cells, as well as unstained samples from the same kidneys were negative (Figure 5d). Immunoelectron microscopy confirmed VEGFR2 protein expression

in podocyte foot processes and cell bodies as well as in endothelial cells (Figure 5e and f). Tyrosine phosphorylated VEGFR2 was detected in glomeruli from control mice but rarely colocalized with nephrin (Figure 5g, −dox), whereas phosphorylated VEGFR2 was increased and colocalized with nephrin in podocytes from $VEGF_{164}$-overexpressing mice (Figure 5g, + dox), suggesting that increased $VEGF_{164}$ signals induced VEGFR2 phosphorylation in podocytes.

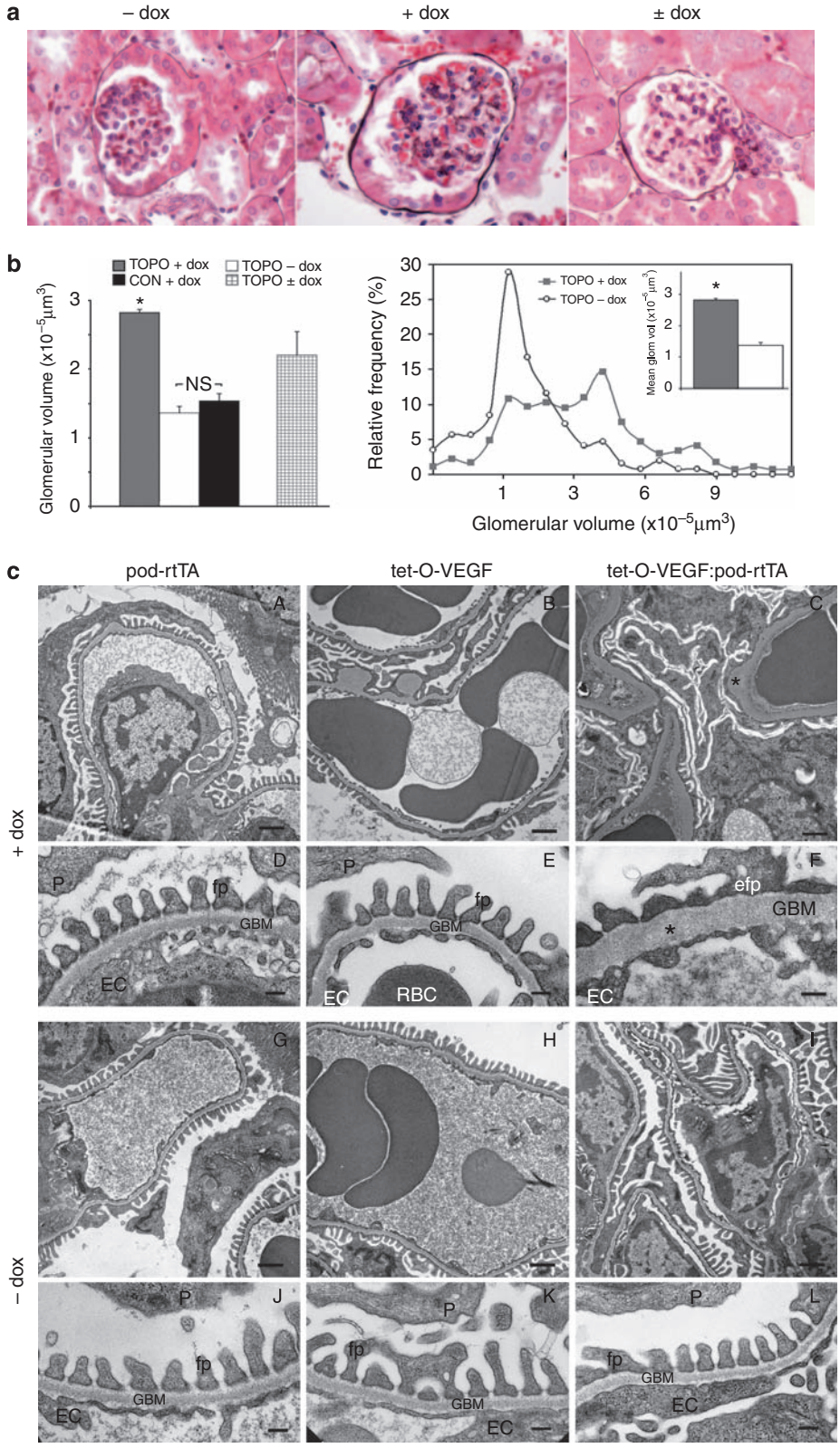

To examine a possible crosstalk between VEGF-A and nephrin signaling pathways we performed immunoprecipitation experiments. VEGFR2 co-immunoprecipitated with nephrin in kidney lysates (Figure 5h), indicating that VEGFR2 and nephrin interact *in vivo*. Moreover, purified FLAG-tagged VEGFR2 protein associated with endogenous nephrin (Figure 5i), confirming the interaction *in vitro*. Together, our findings show that VEGFR2 is expressed in podocytes and interacts with nephrin *in vivo*, suggesting that the phenotype induced by podocyte $VEGF_{164}$ overexpression results from autocrine and paracrine signals, which involve nephrin and MMP-9 dysregulation, nephrin–VEGFR2 interaction, and $VEGF_{164}$-induced phosphorylation of both proteins *in vivo*.

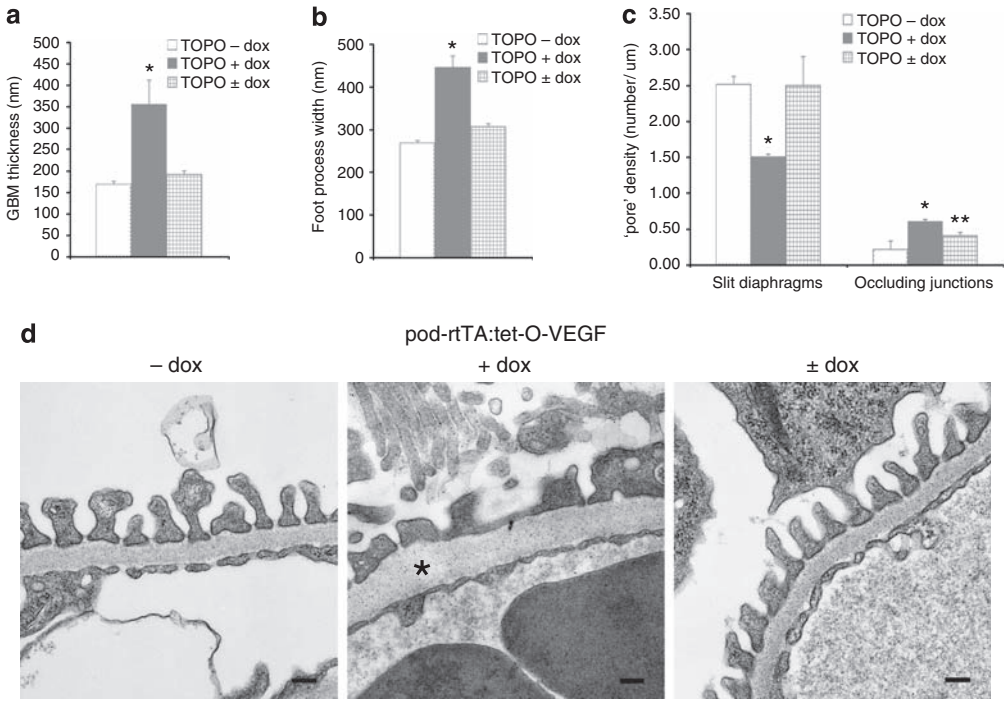

Figure 3 | Ultrastructural abnormalities caused by podocyte $VEGF_{164}$ overexpression are reversible. Morphometric comparisons were made among *podocin-rtTA:tet-O-VEGF*$_{164}$ mice uninduced, induced, and that in which induction was removed to test reversibility (TOPO −dox, TOPO + dox, and TOPO ± dox, respectively). (**a**) Glomerular basement membrane (GBM) thickness expressed in nm, showing a twofold increase in mice overexpressing $VEGF_{164}$; (**b**) foot process width, a measure of podocyte effacement, increased >60% in mice overexpressing $VEGF_{164}$; (**c**) density of podocyte foot process interactions ('pores'), measured as the number of slit diaphragms (SD) or occluding junctions (OJ) per μm of GBM length, showing mirror image changes: increase in OJ and decrease in SD in mice overexpressing $VEGF_{164}$. Changes in all these morphometric parameters were reversible upon removal of $VEGF_{164}$ induction (TOPO ± dox). Total number of measurements (*n*) for each parameter in TOPO −dox, TOPO + dox, and TOPO ± dox mice were as follows: GBM thickness: $n = 241$, 431, and 272; foot process width: $n = 422$, 584, and 311; SD: $n = 378$, 409, and 254; and OJ: $n = 32$, 165, and 40. *$P < 0.05$, TOPO + dox vs TOPO −dox or TOPO ± dox; **$P < 0.05$, TOPO ± dox vs TOPO −dox. (**d**) Representative transmission electron microscopy (TEM) showing the reversible ultrastructural abnormalities quantified in (**a–c**), large * points out the thickened GBM. Notice the lack of endothelial cell abnormalities, scale bars = 200 nm.

Figure 2 | Podocyte $VEGF_{164}$ overexpression in adult mice causes glomerulomegaly, GBM thickening, podocyte effacement, and SD loss. (**a**) Gomorri's silver methenamine stain in *podocin-rtTA:tet-O-VEGF*$_{164}$ uninduced mice (TOPO −dox), mice induced for 1 month (TOPO + dox), and mice induced for 1 month, and then off induction for 2 weeks (TOPO ± dox), showing enlarged glomeruli with thicker GBM in TOPO + dox mice, and regression of these changes in TOPO ± dox mice. (**b**) Morphometric analysis of glomerular size: *podocin-rtTA:tet-O-VEGF*$_{164}$ induced mice (TOPO + dox) had approximately twofold larger glomerular volume than uninduced mice (TOPO −dox) and controls (CON + dox); the glomerular enlargement partially subsided after 2 weeks off doxycycline (TOPO ± dox). The distribution of glomerular volumes showed significantly increased size heterogeneity in induced mice (TOPO + dox), in addition to overall enlargement, as shown by the mean ± s.e.m. difference (inset). *$P < 0.05$, TOPO + dox vs TOPO −dox-treated mice. (**c**) TEM showing kidneys from podocin-rtTA mice (left panels), *tet-O-VEGF*$_{164}$ mice (middle panels), and *podocin-rtTA:tet-O-VEGF*$_{164}$ mice (right panels) induced with doxycycline for 1 month (+ dox), and uninduced (−dox). All left and middle panels (single transgenics) show normal kidney ultrastructure, whereas induced *podocin-rtTA:tet-O-VEGF*$_{164}$ kidneys (top panels C and F) show diffuse GBM thickening (*), mesangial expansion, and podocyte effacement. Notice that uninduced *podocin-rtTA:tet-O-VEGF*$_{164}$ kidneys are normal (bottom panels I and L). Scale bars = 1 μm in panels A–C and G–I, and = 200 nm in panels D–F and J–L. EC, endothelial cell; efp, effaced foot process, fp, foot process; GBM, glomerular basement membrane; P, podocyte; RBC, red blood cell; SD, slit diaphragm; TEM, transmission electron microscopy.

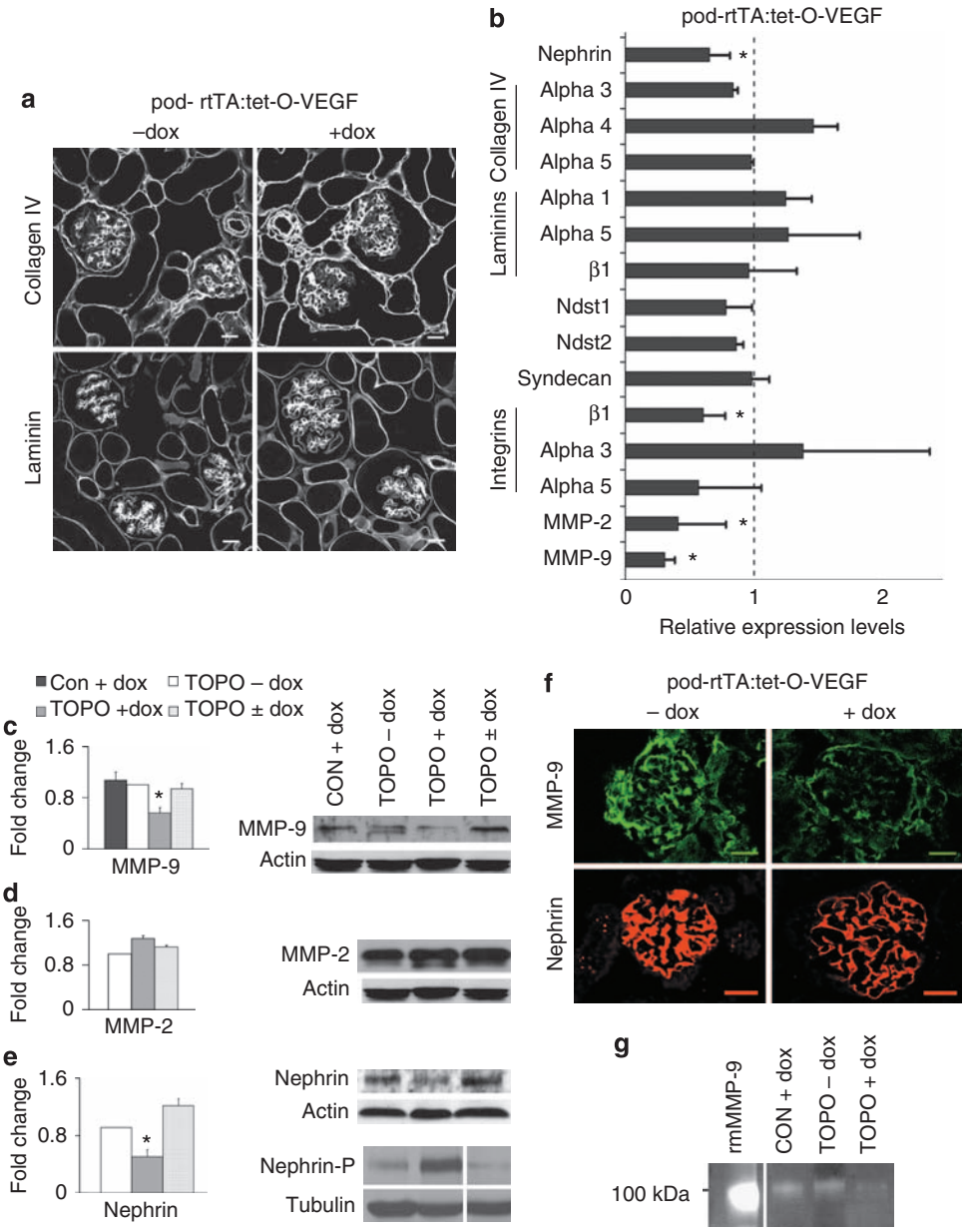

Figure 4 | Podocyte $VEGF_{164}$ induction in adult mice decreases matrix metalloproteinase 9 (MMP-9) and nephrin. (**a**) Fluorescent immunohistochemistry showing that collagen IV and laminin are normally localized in mice overexpressing $VEGF_{164}$. (**b**) Real-time PCR data showing relative mRNA expression of glomerular basement membrane (GBM) components and nephrin in mice overexpressing $VEGF_{164}$/uninduced mice of the same genotype (TOPO + dox/ TOPO −dox), using pooled RNA from 9 and 8 mice, respectively. Data are expressed as mean fold changes ± s.e.m., $n = 3$, $^*P < 0.05$. (**c**) Western blot showing decreased MMP-9 protein in mice overexpressing $VEGF_{164}$ (TOPO + dox) vs uninduced mice (TOPO −dox), controls are single transgenic on dox (CON + dox), MMP-9 downregulation is reversible (TOPO ± dox). (**d**) Western blot showing no change in MMP-2 levels in TOPO + dox, TOPO −dox, and TOPO ± dox. (**e**) Western blots showing decreased nephrin expression and enhanced phosphorylation in $VEGF_{164}$-overexpressing (TOPO + dox) vs uninduced kidneys (TOPO −dox), nephrin dysregulation is reversible (TOPO ± dox). In (**c–e**) whole kidney lysate was pooled from 13 (TOPO + dox) and 8 (TOPO −dox) *podocin-rtTA:tet-O-VEGF$_{164}$* mice, 8 single transgenic mice (CON + dox), and 6 *podocin-rtTA:tet-O-VEGF$_{164}$* mice on doxycycline for 1 month and off for 2 weeks (TOPO ± dox). Actin and tubulin blots are shown to document equal loading. Densitometric analysis shows mean ± s.e.m. fold change in arbitrary units when compared with controls, $n \geqslant 4$. (**f**) MMP-9 and nephrin immunohistochemistry. *Podocin-rtTA:tet-O-VEGF$_{164}$* induced (+dox) showed decreased MMP-9 and nephrin when compared with uninduced mice (−dox), with unchanged localization, scale bars = 20 μm. (**g**) MMP-9 zymogram shows decreased MMP-9 activity in kidneys overexpressing $VEGF_{164}$ (TOPO + dox), positive control = recombinant mouse MMP-9 (2.5 ng).

DISCUSSION

In this study we show that podocyte $VEGF_{164}$ overexpression in adult mice results in proteinuria and a distinct glomerular phenotype characterized by glomerulomegaly, mesangial expansion, podocyte foot process effacement, and thickened GBM. The cause-and-effect relationship between podocyte $VEGF_{164}$ overexpression and glomerular phenotype was clearly shown by the reversibility of the functional,

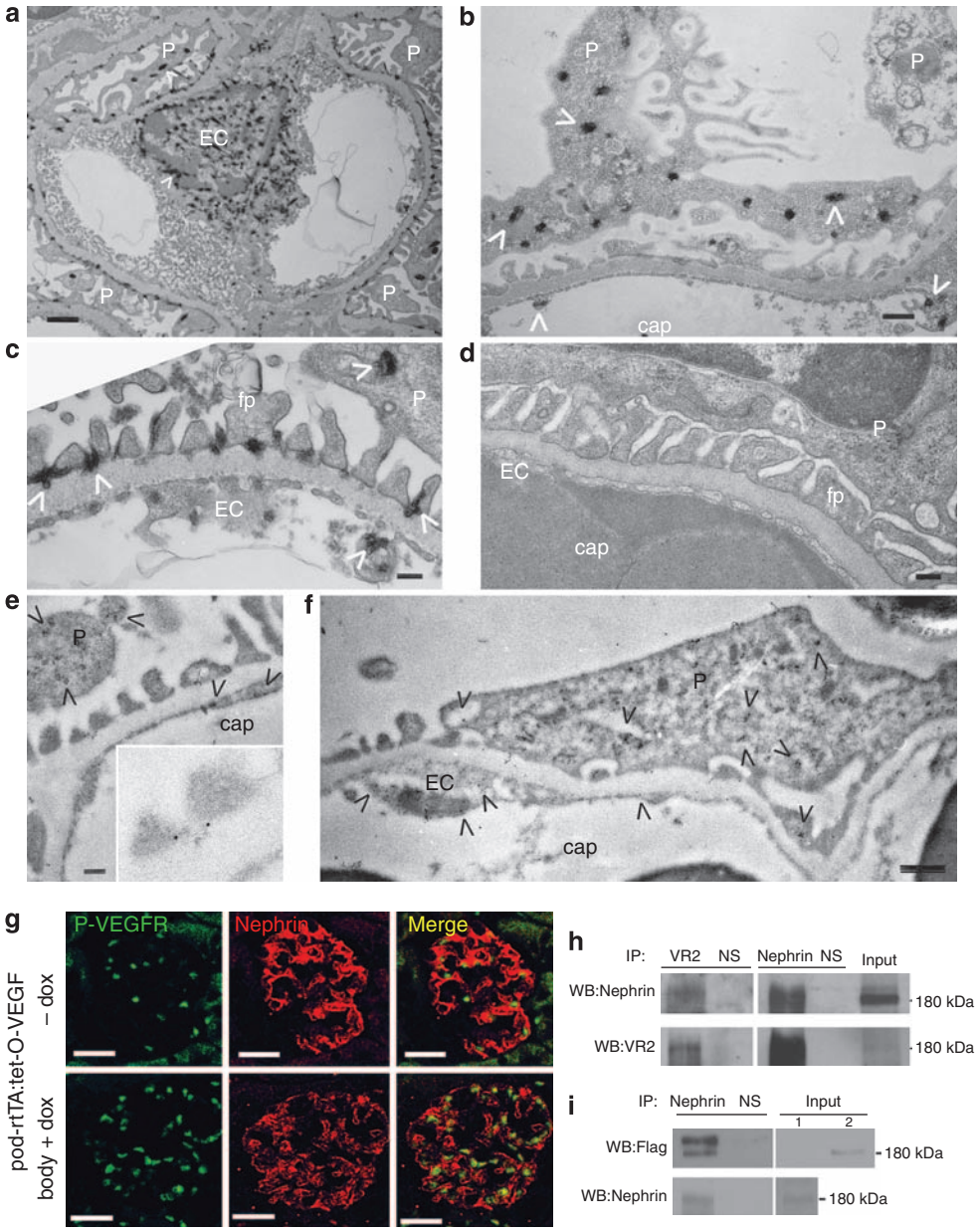

Figure 5 | Vascular endothelial growth factor receptor-2 (VEGFR2) is expressed in podocytes and endothelial cells. (**a**) Transmission electron microscopy (TEM) of LacZ-stained kidneys from adult *Flk-1*$^{+/-}$ LacZ mice showing extensive β-Gal electron-dense deposits in glomerular capillaries and in podocytes, scale bar = 1 μm; (**b**) β-Gal electron deposits in a podocyte body, scale bar = 500 nm; and (**c**) β-Gal electron deposits in foot processes, scale bar = 200 nm. (**d**) TEM of the same kidney, not stained for LacZ (negative control), scale bar = 200 nm. (**e**) Immunogold staining for VEGFR2 showing immunoreactive VEGFR2 in foot processes, scale bar = 200 nm, inset: higher magnification of two foot processes flanking a slit diaphragm showing immunogold VEGFR2 staining; (**f**) immunoreactive VEGFR2 in podocyte body and endothelial cell, scale bar = 500 nm. cap, capillary lumen; EC, endothelial cell; fp, foot process; P, podocyte. ^β Gal electron-dense deposits. (**g**) $VEGF_{164}$ overexpression induces VEGFR2 phosphorylation in podocytes: immunoreactive phosphorylated (P)-VEGFR2 (green) is increased in glomeruli from $VEGF_{164}$-overexpressing mice (+dox) as compared with uninduced glomeruli (−dox); nephrin (red) and P-VEGFR2 (green) colocalize (yellow) in podocytes from $VEGF_{164}$-overexpressing mice (+dox). Scale bars = 20 μm. (**h**) VEGFR2 and nephrin interact *in vivo*: immunoprecipitation (IP) with anti-VEGFR2 (VR2) antibody followed by western blotting (WB) with anti-nephrin antibody and VEGFR2 antibody showing co-immunoprecipitation; reverse co-IP experiment: IP with anti-nephrin antibody, followed by WB with anti-nephrin and anti-VEGFR2 antibody; VR2, VEGFR2; NS, normal rabbit serum (IP negative control); input, whole kidney lysate. (**i**) VEGFR2 and nephrin interact *in vitro*: IP with anti-nephrin, followed by WB with anti-Flag and anti-nephrin antibodies, showing that nephrin immunoprecipitate interacts with purified Flag-tagged VEGFR2; input 1, whole kidney lysate; input 2, Flag-VEGFR2 transfected COS cell lysate.

morphologic, and molecular changes observed upon removal of doxycycline.

Podocyte $VEGF_{164}$ overexpression-induced albuminuria was 4- to 16-fold higher than control, the proteinuria had a significant positive correlation with the kidney VEGF-A content, and most importantly, was fully reversible upon cessation of doxycycline. The association of glomerulomegaly, mildly increased mesangial matrix, GBM thickening,

and foot process widening with loss of slit diaphragms induced by podocyte $VEGF_{164}$ overexpression in adult mice were similar to the classic glomerular abnormalities reported in early diabetic nephropathy in humans and rodents.[18,21] However, normal glucose levels in mice overexpressing podocyte $VEGF_{164}$ ruled out diabetes mellitus, and the absence of hypertension ruled out $VEGF_{164}$-induced hypertensive nephrosclerosis.

The dramatic GBM thickening and the lack of significant endothelial cell damage observed by TEM in adult mice overexpressing podocyte $VEGF_{164}$ clearly differ from the glomerular phenotypes described in VEGF-induced collapsing glomerulopathy,[4] and a rabbit model of liver and kidney VEGF overexpression,[22] probably because of timing of VEGF overexpression, transgene dosage, and species differences. Our data show pathogenic effects of moderately increased podocyte $VEGF_{164}$ in adult mice causing a distinct GBM and podocyte phenotype that spares the glomerular endothelial cells. Furthermore, we show that the molecular mechanism responsible for this phenotype involves decreased expression of collagenase MMP-9 and nephrin.

We provide evidence of decreased MMP-9 expression and activity in podocyte $VEGF_{164}$-overexpressing mice. As doxycycline is a known inhibitor of metalloproteinases,[19,23] we also examined the effect of doxycycline on renal MMP-2 and MMP-9 expression in single transgenic mice. We determined that downregulation of MMP-9 expression is clearly induced by $VEGF_{164}$ overexpression, as it was abrogated by removal of $VEGF_{164}$ transgene induction, and remained stable in all control mice receiving doxycycline. Surprisingly, MMP-2 protein expression levels were not altered in mice overexpressing podocyte $VEGF_{164}$. Taken together, these findings suggest that podocyte $VEGF_{164}$ overexpression *in vivo* reduces GBM turnover, rather than enhancing synthesis of GBM components such as collagen IV and perlecan, as suggested by *in vitro* data.[24,25] Alternatively, the thickened GBM could be due to deposition of another collagen type not normally expressed in the GBM, such as collagen type III,[18,26,27] but our quantitative reverse transcriptase-PCR data do not support this possibility (data not shown).

Consistent with partial podocyte effacement and fusion, we detected downregulation of nephrin expression and increased nephrin phosphorylation in podocyte $VEGF_{164}$-overexpressing kidneys, which were reversible upon doxycycline removal, suggesting that increased VEGF-A signaling alters the nephrin signaling complex function, and thereby podocyte phenotype. Decreased nephrin expression has been described in multiple human proteinuric diseases,[28,29] including diabetic nephropathy.[18,21,30] Increased nephrin phosphorylation has been observed during development and in a rodent model of foot process effacement,[31] whereas decreased nephrin phosphorylation was reported in rat puromycin aminonucleoside nephrosis and in human minimal change disease.[32] As deletion of Nck, an adaptor protein that selectively binds to phosphorylated nephrin, leads to congenital nephrotic syndrome,[33] it seems that signals mediated by phosphorylated nephrin are necessary for the establishment of mature podocyte foot processes and slit diaphragms, whereas the role of dysregulated nephrin phosphorylation in postnatal glomerular diseases is less clear.

We sought to identify the glomerular cell types expressing VEGFR2, the main VEGF-A signaling receptor,[34–36] to understand whether the ultrastructural abnormalities and the associated nephrin dysregulation observed in podocyte *$VEGF_{164}$*-overexpressing mice were caused by autocrine or paracrine signaling. Using TEM combined with either β-Gal staining[37] or immunogold staining, we detected VEGFR2 expression in glomerular endothelial cells and in podocytes, extensively distributed in the cell body, foot processes, and close to slit diaphgrams. Furthermore, increased activated VEGFR2 was detected by immunohistochemistry in podocytes from mice overexpressing $VEGF_{164}$, suggesting that increased $VEGF_{164}$ signals induced VEGFR2 phosphorylation *in situ*. Localization of VEGFR2, but not VEGFR1, to podocytes by immunogold staining was recently reported.[38]

We identified a novel interaction between endogenous VEGFR2 and nephrin by co-immunoprecipitation *in vivo*, and confirmed the association between purified Flag-tagged mouse VEGFR2 and endogenous nephrin from kidney lysates, suggesting a crosstalk between VEGF-A and nephrin pathways. As nephrin expression is limited to podocytes, this interaction independently confirms the expression of VEGFR2 in podocytes. Moreover, our observation that podocyte $VEGF_{164}$ overexpression induced nephrin phosphorylation supports the notion that VEGFR2–nephrin interaction may have functional relevance, and represents a novel mechanism for crosstalk between VEGF-A and nephrin signaling pathways. Collectively, our findings suggest that podocyte $VEGF_{164}$ signaling is both autocrine and paracrine, and provide a plausible interpretation for the podocyte phenotypic changes and the nephrin dysregulation observed in podocyte $VEGF_{164}$-overexpressing kidneys. Further studies are warranted to define the biochemistry of VEGFR2–nephrin interaction, and how it modulates nephrin signaling. As *Flk-1*-null mice are embryonic lethal and heterozygous mice do not have a vascular or glomerular phenotype,[20] only a complete, inducible, and podocyte-specific *VEGFR2* knockout would definitively elucidate whether the mechanism proposed in this study is required for the integrity of the glomerular filtration barrier. Our studies do not exclude possible effects of $VEGF_{164}$ overexpression through VEGFR1, which is considered to exert an effect as a negative modulator of VEGFR2 signaling in most tissues by sequestering VEGF-A ligand, and thereby decreasing VEGFR2 activation, although the mechanisms involved remain controversial.[34–36]

In summary, induction of podocyte $VEGF_{164}$ overexpression in the adult mouse causes proteinuric glomerular disease that mimics early diabetic nephropathy, in the absence of a diabetic milieu. Reversibility of these changes upon removal of doxycycline provides proof of principle of the causal relationship. Our findings are consistent with an autocrine pathogenic role of increased podocyte VEGF-A in this

process, involving nephrin and MMP-9 dysregulation, nephrin–VEGFR2 interaction, and $VEGF_{164}$-induced phosphorylation of both proteins *in vivo*. Our inducible model should prove useful to identify the downstream mechanisms of VEGF-induced glomerular disease in adult mice, and to test therapeutic interventions.

MATERIALS AND METHODS

Inducible, podocyte-specific $VEGF_{164}$ overexpression in mice

All mouse protocols were approved by the Committee for Animal Use and Experimentation of Albert Einstein College of Medicine. We generated tetracycline-regulated transgenic mice (*podocin-rtTA:tet-O-$VEGF_{164}$*) that overexpress VEGF-A in podocytes upon induction with doxycycline by breeding *podocin-rtTA* mice[16] with *tet-O-$VEGF_{164}$* mice,[17] which carry FVB background. Transgenic mice were genotyped by reverse transcriptase-PCR using reported primers.[16,17] Adult *podocin-rtTA:tet-O-$VEGF_{164}$* mice (2–3 months old) received doxycycline (0.625 mg/g chow, Harlen-Teklar, Madison, WI, USA) for 1 month (TOPO +dox, $n=14$). Uninduced *podocin-rtTA:tet-O-$VEGF_{164}$* (TOPO −dox, $n=9$), induced single transgenics (CON +dox, $n=4$), and uninduced single transgenics (CON −dox, $n=4$) served as controls. Additional *podocin-rtTA:tet-O-$VEGF_{164}$* mice were induced with doxycycline for 1 month, and then switched to regular diet for 2 weeks to examine the reversibility of $VEGF_{164}$-induced changes (TOPO ± dox, $n=6$). Blood pressure was measured using the Coda Noninvasive-Blood-Pressure-System (Kent Scientific, Torrington, CT, USA).[39]

Proteinuria and VEGF-A analysis

Mice were anesthetized with ketamine, and blood and urine samples were obtained from venous and bladder puncture, kidneys were harvested for phenotype analysis, and mice were then killed by exsanguination. Urinary creatinine was measured using a colorimetric assay (Oxford Biomedical Research, Oxford, MI, USA). Albuminuria was assessed by dipstick (Albustix; Bayer, Elkhart, IN, USA), enzyme-linked immunosorbent assay (Albuwell; Exocell, Philadelphia, PA, USA), and immunoblotting. Urine samples (normalized for creatinine) were resolved by sodium dodecyl sulfate-polyacrylamide gel electrophoresis and immunoblotted with anti-bovine serum albumin antibody (Upstate Biotechnology, Lake Placid, NY, USA). Serum and whole kidney VEGF-A were measured by enzyme-linked immunosorbent assay (mVEGF-A, R&D, Minneapolis, MN, USA), following the manufacturer's protocol. Serum glucose was measured by glucose oxidase biosensor (One-Touch-Ultra-2 Blood Glucose-Meter, LifeScan, Milpitas, CA, USA).

Histology and morphometry

Kidneys were processed for light and transmission electron microscopy or frozen in isopentane and mounted in optimum cutting temperature compound (Sakura, Torrance, CA, USA). Hematoxylin/eosin and Gomorri's silver methenamine staining were performed.

Morphometric analysis. Glomerular diameters were measured in 135 ± 5 gloms/section at ×400 magnification. Glomerular volume was determined as $Gv=\beta/k.(\pi.r^2)^{3/2}$, where $\beta=1.38$ is the shape coefficient for spheres, $k=1.1$ is the size distribution coefficient, and $(\pi.r^2)$ is the glomerular area.[26] Measurements were carried out in four mice per group. Slit diaphragms, foot process width, and GBM thickness were measured on TEM scans using Image J, Bethesda, MD, USA (NIH). Measurements were made perpendicular to the axis of the GBM every 500 nm on 30–50 μm GBM length/5K images. Occluding junctions and slit diaphragms were counted and normalized to GBM length (μm), termed 'OJ or SD density'. TEM measurements were carried out in five mice per group; counts for each parameter are depicted in figure legends.

Immunohistochemistry

Kidneys were embedded in optimum cutting temperature compound, and snap-frozen in dry ice/isopentane or fixed in formalin and paraffin embedded. Paraffin sections were deparaffinized, incubated in 10 mM citrate, blocked, and incubated with anti-VEGF antibody (Dako, Carpinteria, CA, USA, M7273), anti-nephrin (Fitzgerald, North Acton, MA, USA, 20R-NP002), and anti-phospho-$VEGFR2^{tyr1175}$ (Cell Signaling, Danvers, MA, USA, 19A10). Bound primary antibodies were visualized by immunoperoxidase (Dako EnVision + System), counterstained with hematoxylin, or by fluorescent-labeled (Cy2 or Cy3, Jackson Immunoresearch, West Grove, PA, USA) secondary antibodies. Cryosections (6 μm) were fixed in cold acetone, permeabilized with 0.3% Triton-X, blocked, and incubated with primary antibodies: anti MMP-9 (ab38898, Abcam, Cambridge, MA, USA), anti-podocin (gift from P. Mundel, University of Miami School of Medicine), anti-collagen IV (Southern Biotech, Birmingham, AL, USA) and anti-laminin (Sigma, St Louis, MD, USA), followed by appropriate Cy2- or Cy3-labeled anti-rabbit, anti-mouse, or anti-goat secondary antibodies. All sections were examined by confocal microscopy (FV300, Olympus, Center Valley, PA, USA).

Transmission electron microscopy, β-Gal stain, and immunoelectron microscopy

Kidney cortex was minced to 2 mm cubes, fixed with 2% paraformaldehyde, 2.5% glutaraldehyde in 0.1 M sodium-cacodylate buffer, postfixed with 1% OsO_4 followed by 2% uranyl acetate, dehydrated through a graded series of ethanol, and embedded in LX112 (Ladd Research, Williston, VT, USA). Thin sections (80 nm) were cut and stained with 0.5% uranyl acetate and 0.5% lead citrate. For TEM β-Gal stain, kidneys were fixed and processed for LacZ stain as described,[20] postfixed as above, and processed for TEM using standard techniques, except that uranyl acetate and lead citrate steps were omitted, as they obscure the detection of β-Gal precipitates.[37] For immunogold labeling, kidneys were fixed with 4% paraformaldehyde and 0.05% glutaraldehyde in 0.1 M sodium cacodylate buffer and subsequently processed as for TEM and embedded in LR-white resin (London Resin Co, Basingstoke, UK). Sections were blocked with 0.05 M glycine, followed by goat blocking buffer (Aurion, Nl), incubated with anti-VEGFR2 polyclonal antibody (SC no. 315 or SC no. 504, Santa Cruz, CA, USA), incubated with 10 nm goat anti-rabbit gold (Aurion, Wageningen, The Netherlands), counterstained with 0.5% uranyl acetate and 0.5% lead citrate, and examined using a JEOL 1200EX TEM (Tokyo, Japan).

Real-time PCR

Total RNA was isolated from whole kidney cortex from *podocin-rtTA:tet-O-$VEGF_{164}$* mice receiving doxycycline (TOPO +dox, $n=9$) or not (TOPO −dox, $n=8$ age-matched) using Trizol Reagent (Invitrogen, Carlsbad, CA, USA). After DNAse digestion, reverse transcription was performed using Quantitect Reverse Transcription Kit (Qiagen, Valencia, CA, USA). Reverse transcription products were combined into separate pools (TOPO +dox and TOPO −dox). Real-time PCR amplifications were performed using SYBR-Green PCR-Master-Mix (Applied Biosystems, Foster City, CA, USA), appropriate primers (Supplementary Table 1), and an

Eppendorf Realplex2 Mastercycler (Hamburg, Germany). The cycle threshold (Ct) of amplified products was detected using the manufacturer's software. Samples were run in duplicate and experiments were repeated a minimum of three times. Relative quantification was determined using the ΔCt method.[40] Data were normalized to glyceraldehyde-3-phosphate dehydrogenase and expressed as fold change relative to uninduced *podocin-rtTA:tet-O-VEGF$_{164}$* mice (TOPO +dox/TOPO −dox).

Immunoblotting, immunoprecipitation, and zymogram

Kidneys from age-matched *podocin-rtTA:tet-O-VEGF$_{164}$* mice receiving doxycycline (TOPO +dox, $n=13$) or not (TOPO −dox, $n=8$) were lysed in RIPA buffer + protease inhibitors (Roche, Indianapolis, IN, USA) +1 mM Na_3VO_4 +1 mM NaF. Protein concentration was determined by bicinchoninic acid assay (Sigma). Equal amount of protein lysate from individual kidneys were combined into separate pools (+dox and −dox), and 100–150 μg protein/lane were resolved in 8–15% sodium dodecyl sulfate-polyacrylamide gel electrophoresis. Primary antibodies used for immunoblotting were: anti-nephrin (20R-NP002, Fitzgerald); anti-phosphorylated nephrin;[31] anti-MMP-2 (Chemicon, Billerica, MA, USA); and anti-MMP-9 (Chemicon). Anti-actin (A2066, Sigma) or anti-tubulin (sc-58667, Santa Cruz) was used as a control for protein loading. For nephrin and VEGFR2 immunoprecipitation experiments, 1 mg protein from whole kidney lysate was resuspended in immunoprecipitation buffers as described,[31,41] with slight modifications (1% Triton X-100, 1% NP-40, 0.5% deoxycholate, 10 mM Tris, pH 8, 0.15 M NaCl, 1 mM EDTA, 50 mM NaF and 1 mM Na_3VO_4, protease inhibitor cocktail), pre-cleared, and incubated with polyclonal nephrin[31] and VEGFR2 (sc-504, Santa Cruz) antibodies. Some nephrin immunoprecipitation experiments were followed by overnight incubation with 1 μg Flag-VEGFR2 protein purified from COS cells transfected with Flag-mouse VEGFR2, immunoblotted, and VEGFR2 was detected by anti-Flag monoclonal antibody (Sigma). Rabbit serum was used as negative control. Lysates from COS cells and whole kidney were used as positive controls. Secondary antibodies were anti-rabbit or anti-mouse-horseradish peroxidase-IgG (Amersham), detected by chemoluminescence (Amersham). Kidney lysate pools (100 μg) were denatured in sodium dodecyl sulfate buffer, resolved in zymogram gels (Novex-Zymogram-Gel; Invitrogen), renatured, developed, and stained following the manufacturer's instructions. Positive control was recombinant mouse MMP-9 (R&D). Gelatinolytic activity revealed clear bands on a blue background.

Statistical analysis

All values are expressed as mean ± s.e.m. To determine statistical significance, we used unpaired Student's *t*-test and one-way analysis of variance for comparisons between two groups or multiple groups, respectively. The Bonferroni correction was used to adjust for multiple testing in quantitative PCR experiments. Mann–Whitney *U*-test was used for albumin:creatinine ratios, as these data did not have a Gaussian distribution. $P<0.05$ was deemed statistically significant.

DISCLOSURE

All the authors declared no competing interests.

ACKNOWLEDGMENTS

We thank A. Akeson and J. Whittsett (Cincinnati Children's Hospital) for providing the *tet-O-VEGF$_{164}$* mice. We thank Lawrence Holzman for providing nephrin antibodies and thoughtful advice. We thank Frank Macaluso and Leslie Cummings (AECOM Imaging Facility) for technical assistance with TEM. Portions of this work were presented at the 2007 ASN meeting. This study was supported by the NIH RO1 DK59333 and O'Brien Center Grant P50 DK64236 (to AT). KJR was supported by the NIH training Grant T32 DK 007110. NIDDK intramural research program (to JBK).

SUPPLEMENTARY MATERIAL

Figure S1. Tetracycline-regulated inducible podocyte VEGF$_{164}$ overexpression in adult mice.
Figure S2. Podocyte VEGF$_{164}$ overexpression in adult mice causes mild mesangial expansion.
Table S1. PCR primers

Supplementary material is linked to the online version of the paper at http://www.nature.com/ki

REFERENCES

1. Coultas L, Chawengsaksophak K, Rossant J. Endothelial cells and VEGF in vascular development. *Nature* 2005; **438**: 937–945.
2. Carmeliet P, Ferreira V, Breier G *et al.* Abnormal blood vessel development and lethality in embryos lacking a single VEGF allele. *Nature* 1996; **380**: 435–439.
3. Ferrara N, Carver-Moore K, Chen H *et al.* Heterozygous embryonic lethality induced by targeted inactivation of the VEGF gene. *Nature* 1996; **380**: 439–442.
4. Eremina V, Cui S, Gerber H *et al.* Glomerular-specific alterations of VEGF-A expression lead to distinct congenital and acquired renal diseases. *J Clin Invest* 2003; **111**: 707–716.
5. Schrijvers BF, Flyvbjerg A, De Vriese AS. The role of vascular endothelial growth factor (VEGF) in renal pathophysiology. *Kidney Int* 2004; **65**: 2003–2017.
6. Quaggin SE, Coffman TM. Toward a mouse model of diabetic nephropathy: is endothelial nitric oxide synthase the missing link? *J Am Soc Nephrol* 2007; **18**: 364–367.
7. Cooper ME, Vranes D, Youssef S *et al.* Increased renal expression of vascular endothelial growth factor (VEGF) and its receptor VEGFR-2 in experimental diabetes. *Diabetes* 1999; **48**: 2229–2239.
8. De Vriese AS, Tilton RG, Elger M *et al.* Antibodies against vascular endothelial growth factor improve early renal dysfunction in experimental diabetes. *J Am Soc Nephrol* 2001; **12**: 993–1000.
9. Flyvbjerg A, Dagnaes-Hansen F, De Vriese AS *et al.* Amelioration of long-term renal changes in obese type 2 diabetic mice by a neutralizing vascular endothelial growth factor antibody. *Diabetes* 2002; **51**: 3090–3094.
10. Sung SH, Ziyadeh FN, Wang A *et al.* Blockade of vascular endothelial growth factor signaling ameliorates diabetic albuminuria in mice. *J Am Soc Nephrol* 2006; **17**: 3093–3104.
11. Eremina V, Jefferson JA, Kowalewska J *et al.* VEGF inhibition and renal thrombotic microangiopathy. *N Engl J Med* 2008; **358**: 1129–1136.
12. Gurevich F, Perazella MA. Renal effects of anti-angiogenesis therapy: update for the internist. *Am J Med* 2009; **122**: 322–328.
13. Nakagawa T. Uncoupling of the VEGF-endothelial nitric oxide axis in diabetic nephropathy: an explanation for the paradoxical effects of VEGF in renal disease. *Am J Physiol Renal Physiol* 2007; **292**: F1665–F1672.
14. Tufró A. VEGF spatially directs angiogenesis during metanephric development *in vitro*. *Dev Biol* 2000; **227**: 558–566.
15. Guan F, Villegas G, Teichman J *et al.* Autocrine VEGF-A system in podocytes regulates podocin and its interaction with CD2AP. *Am J Physiol* 2006; **291**: F422–F428.
16. Shigehara T, Zaragoza C, Kitiyakara C *et al.* Inducible podocyte-specific gene expression in transgenic mice. *J Am Soc Nephrol* 2003; **14**: 1998–2003.
17. Akeson AL, Greenberg JM, Cameron JE *et al.* Temporal and spatial regulation of VEGF-A controls vascular patterning in the embryonic lung. *Dev Biol* 2003; **264**: 443–455.
18. Fioretto P, Mauer M. Histopathology of diabetic nephropathy. *Semin Nephrol* 2007; **27**: 195–207.
19. Raffetto JD, Khalil RA. Matrix metalloproteinases and their inhibitors in vascular remodeling and vascular disease. *Biochem Pharmacol* 2008; **75**: 346–359.
20. Shalaby F, Rossant J, Yamaguchi TP *et al.* Failure of blood-island formation and vasculogenesis in Flk-1-deficient mice. *Nature* 1995; **376**: 62–66.

21. Breyer MD, Böttinger E, Brosius 3rd FC *et al.* AMDCC: mouse models of diabetic nephropathy. *J Am Soc Nephrol* 2005; **16**: 27–45.
22. Liu E, Morimoto M, Kitajima S *et al.* Increased expression of vascular endothelial growth factor in kidney leads to progressive impairment of glomerular functions. *J Am Soc Nephrol* 2007; **18**: 2094–2104.
23. Castro MM, Rizzi E, Figueiredo-Lopes L *et al.* Metalloproteinase inhibition ameliorates hypertension and prevents vascular dysfunction and remodeling in renovascular hypertensive rats. *Atherosclerosis* 2008; **198**: 320–331.
24. Chen S, Kasama Y, Lee JS *et al. Diabetes* 2004; **53**: 2939–2949.
25. Kaji T, Yamamoto C, Oh-i M *et al.* The vascular endothelial growth factor $VEGF_{165}$ induces perlecan synthesis via VEGF receptor-2 in cultured human brain microvascular endothelial cells. *Biochem Biophys Acta* 2006; **1760**: 1465–1474.
26. Hirose K, Osterby R, Nozawa M *et al.* Development of glomerular lesions in experimental long-term diabetes in the rat. *Kidney Int* 1982; **21**: 689–695.
27. Nerlich A, Schleicher E. Immunohistochemical localization of extracellular matrix components in human diabetic glomerular lesions. *Am J Pathol* 1991; **139**: 889–899.
28. Koop K, Eikmans M, Baelde HJ *et al.* Expression of podocyte-associated molecules in acquired human kidney diseases. *J Am Soc Nephrol* 2003; **14**: 2063–2071.
29. Kalluri R. Proteinuria with and without renal glomerular podocyte effacement. *J Am Soc Nephrol* 2006; **17**: 2383–2389.
30. Benigni A, Gagliardini E, Tomasoni S *et al.* Selective impairment of gene expression and assembly of nephrin in human diabetic nephropathy. *Kidney Int* 2004; **65**: 2193–2000.
31. Verma R, Kovari I, Soofi A *et al.* Nephrin ectodomain engagement results in Src kinase activation, nephrin phosphorylation, Nck recruitment, and actin polymerization. *J Clin Invest* 2006; **116**: 1346–1359.
32. Uchida K, Suzuki K, Iwamoto M *et al.* Decreased tyrosine phosphorylation of nephrin in rat and human nephrosis. *Kidney Int* 2008; **73**: 926–932.
33. Jones N, Blasutig IM, Eremina V *et al.* Nck adaptor proteins link nephrin to the actin cytoskeleton of kidney podocytes. *Nature* 2006; **440**: 818–823.
34. Ferrara N, Gerber HP, LeCouter J. The biology of VEGF and its receptors. *Nat Med* 2006; **6)**: 669–676.
35. Zeng H, Dvorak HF, Mukhopadhyay D. Vascular permeability factor (VPF)/vascular endothelial growth factor (VEGF) receptor-1 down-modulates VPF/VEGF receptor-2- mediated endothelial cell proliferation, but not migration, through phosphatidylinositol 3- kinase-dependent pathways. *J Biol Chem* 2001; **276**: 26969–26979.
36. Olsson AK, Dimberg A, Kreuger J *et al.* VEGF receptor signaling – in control of vascular function. *Nat Rev Mol Cell Biol* 2006; **7**: 359–371.
37. Kosaras B, Snyder E. Electron microscopy and lac-Z labeling. *Methods Mol Biol* 2002; **198**: 157–175.
38. Ku CH, White KE, Dei Cas A *et al.* Inducible overexpression of sFlt-1 in podocytes ameliorates glomerulopathy in diabetic mice. *Diabetes* 2008; **57**: 2824–2833.
39. Fitch RM, Rutledge JC, Wang YX *et al.* Synergistic effect of angiotensin II and nitric oxide synthase inhibitor in increasing aortic stiffness in mice. *Am J Physiol Heart Circ Physiol* 2006; **290**: H1190–H1198.
40. Giulietti A, Overbergh L, Valckx D *et al.* An overview of real-time quantitative PCR: applications to quantify cytokine gene expression. *Methods* 2001; **25**: 386–401.
41. Tufro A, Teichman J, Villegas G. Crosstalk between VEGF-A/VEGFR2 and GDNF/RET signaling pathways. *Biochem Biophys Res Commun* 2007; **358**: 410–416.